HHS Public Access

Author manuscript

Nat Neurosci. Author manuscript; available in PMC 2016 March 01.

Published in final edited form as:

Nat Neurosci. 2015 September ; 18(9): 1256–1264. doi:10.1038/nn.4069.

LSD1n is a H4K20 demethylase regulating memory formation via transcriptional elongation control

Jianxun Wang[1,*], **Francesca Telese**[1,*], **Yuliang Tan**[1,*], **Wenbo Li**[1], **Chunyu Jin**[1], **Xin He**[2], **Harihar Basnet**[1], **Qi Ma**[1], **Daria Merkurjev**[1], **Xiaoyan Zhu**[1], **Zhijie Liu**[1], **Jie Zhang**[1], **Kenny Ohgi**[1], **Havilah Taylor**[1], **Ryan R. White**[3], **Todd S. Macfarlan**[4], **Samuel L. Pfaff**[5], and **Michael G. Rosenfeld**[1]

[1]Howard Hughes Medical Institute, Department of Medicine, University of California, San Diego, 9500 Gilman Drive, La Jolla, CA 92093-0648

[2]Beijing University of Chinese Medicine

[3]Department of Genetics, Albert Einstein College of Medicine

[4]National Institute of Child Health and Human Development

[5]Howard Hughes Medical Institute, Gene Expression Laboratory, The Salk Institute for Biological Studies, 10010 North Torrey Pine Road, La Jolla, CA 92037

Abstract

We report that a neuron-specific isoform of LSD1, LSD1n, resulting from an alternative splicing event, acquires a novel substrate specificity targeting histone H4 K20 methylation, both *in vitro* and *in vivo*. Selective genetic ablation of LSD1n leads to deficits in spatial learning and memory, revealing the functional importance of LSD1n in the regulation of neuronal activity-regulated transcription in a fashion indispensable for long-term memory formation. LSD1n occupies neuronal gene enhancers, promoters and transcribed coding regions, and is required for transcription initiation and elongation steps in response to neuronal activity, indicating the crucial role of H4K20 methylation in coordinating gene transcription with neuronal function. This study reveals that the alternative splicing of LSD1 in neurons, associated with altered substrate

Correspondence and requests for materials should be addressed to: Michael G. Rosenfeld, M.D., Tel: 858-534-5858, mrosenfeld@ucsd.edu.

*Contributed equally.

Author Contributions

J.W., F.T., Y.T. and M.G.R. conceived the project. J.W. performed the biochemical characterization of LSD1n, with assistance of C.J., X.H., H.B., Z.L. and X.Z.; J.W. generated the murine genetic models, with assistance of H.T.; F.T. performed all analyses using primary cortical neuronal cultures and helped coordinate all behavioral studies; Y.T. performed GRO-seq experiments and bioinformatics analyses, with assistance of D.M. and Q.M.; W.L. performed GRO-seq experiments; and K.O. and J.Z. performed deep-sequencing experiments. J.W., F.T., Y.T. and M. G. R. wrote the manuscript. All authors reviewed and commented on the manuscript.

Competing financial interests

The authors declare no competing financial interests.

Accession Number

The RNA-seq, GRO-seq and ChIP-seq datasets were deposited at the Gene Expression Omnibus (GEO) under the subseries entry GSE63271. The NCBI Gene Expression Omnibus accession number for MEF2 ChIP-seq dataset is GSE66710.

specificity, serves as an underlying mechanism acquired by neurons to achieve more precise control of gene expression in the complex processes underlying learning and memory.

Introduction

Evidence of the importance of epigenetic mechanisms underlying complex neuronal processes, including learning and memory, is rapidly emerging[1–4]; hence, neuron-specific alternative splicing events affecting the histone modification machinery become an intriguing potential molecular mechanism for the epigenetic control of neuronal gene transcriptional programs involved in synaptic plasticity and cognition. LSD1/KDM1A was initially described as a cofactor of the REST-CoREST complex[5, 6], and was reported to harbor intrinsic enzymatic activity to remove mono- or di- methyl lysine on histone H3 K4 and, in specific circumstances, H3 K9 respectively[7, 8]. While LSD1 can function as a co-repressor of specific transcription factors, such as REST, by removing H3K4 methylation on gene promoters and enhancers, it also has been reported to function as a co-activator of specific transcription factors by removing H3K9 methylation, suggesting that its intrinsic substrate specificity determines its biological function on transcription regulation[7–10]. Recently, a neuronal splicing variant of *LSD1* has been identified, which is dynamically expressed during mammalian brain development and regulates neurite morphogenesis[11]. This initial report suggested that the alternatively spliced *LSD1* isoform in neurons has distinct biological functions compared to its canonical form, even though it adopts a similar structure compared to the canonical LSD1 in association with CoREST and a histone H3 peptide[11].

We investigated the role of the neuronal specific splicing variant of *LSD1* (*LSD1n*) in the regulation of neuronal gene expression programs and in the cognitive functions of learning and memory, based on the generation of a conditional knockout mouse model that specifically deletes *LSD1n*. In this study, we documented impaired transcriptional response to neuronal activity with defects in both initiation and elongation steps in the *LSD1n* knockout cortical neurons. In addition, the behavioral analysis of *LSD1n* knockout mice revealed the essential role of *LSD1n* for spatial learning and long-term memory formation. Intriguingly, the neuron-specific alternatively spliced isoform of LSD1 exhibits novel substrate specificity for histone H4 K20 methylation, suggesting that neuronal specific alternative splicing event is a mechanism underlying the epigenetic regulation of learning and memory processes.

Results

LSD1n functions as a histone H4 K20 methylase *in vitro*

The alternatively spliced exons occur in intron 2 and in intron 8 resulting in the inclusion of a 60nt exon in intron 2 (E2a), which is ubiquitously expressed, or in the inclusion a 12nt exon in intron 8 (E8a), which is observed exclusively in neurons (Fig. 1a and Suppl Fig. S1a)[11]. We refer to *LSD1* without E8a inclusion as *LSD1c* (canonical form, which includes *LSD1* and *LSD1-E2a*), and to *LSD1* with *E8a* inclusion as *LSD1n* (neuronal form, which includes *LSD1-E8a* and *LSD1-E2a&E8a*) respectively. Using mouse embryonic stem cell

(ES) as a model of *in vitro* differentiation, we found that *LSD1n* was absent in undifferentiated ES cells, but its expression was highly induced upon retinoid acid (RA)-induced ES differentiation towards neuronal lineages (Suppl Fig. S1b). Sequence analysis of vertebrates other than mammals revealed that similar alternative splicing events are present in turtle and fish, in which four or six amino acids are included upon exon inclusion (Suppl Fig. S1c), indicating that the alternative splicing of *LSD1* gene is conserved during evolution. Because the *LSD1n* splicing variant has distinct biological functions compared to its canonical form[11], we were intrigued to know if this variant exhibits distinct enzymatic activity towards novel substrates. Therefore, we performed *in vitro* demethylase assays using recombinant LSD1c and LSD1n proteins purified from bacterial cells (Suppl Fig. S1d). Surprisingly, when using core histones as substrates, while LSD1c showed an H3 K4 demethylase activity as expected, recombinant LSD1n lost its intrinsic activity toward H3 K4 methylation, but gained a specific demethylase activity towards histone H4 K20 (Suppl Fig. S1e). In support of our hypothesis that LSD1n specifically removes H4 K20 methylation, we showed that none of the major methylation sites on histone H3 could be used as a substrate (Suppl Fig. S1e). Moreover, when the lysine 685 in the catalytic domain of LSD1n was mutated (LSD1m, K685A mutant), the demethylase activity towards H4 K20 was lost (Suppl Fig. S1f, S1g), implying that LSD1n also used a FAD-dependent mechanism to remove mono- and di-methylation on lysine *in vitro*, as previously reported[7]. Similar H4K20 demethylase activity was observed when nucleosomes were used as substrates in a CoREST-dependent fashion (Fig. 1b). To further characterize the enzymatic activity of LSD1n, we used H3K4me1, H3K4me2, H3K9me1, H3K9me2, H4K20me1 and H4K20me2 peptides as substrates in the *in vitro* demethylase assays (Suppl Fig. S2a, S2b, S2c). Interestingly, LSD1n, although not as robustly as LSD1c, removed methylations on H3K4me1 and H3K4me2 peptides upon adding recombinant CoREST (Suppl Fig. S2a), in accordance with previously reported H3K4 demethylase activity of LSD1n on histone peptides[11]. However, even in the presence of CoREST, the H3K4 demethylase activity of LSD1n was not observed on substrates of core histones or nucleosomes (Fig. 1b and Suppl Fig. S1e). In similar experiments, neither LSD1n nor LSD1c could demethylate the H3K9me1 or H3K9me2 peptides (Suppl Fig. S2b). Furthermore, we show that LSD1n, but not LSD1m or LSD1c, removed the methyl group from the H4K20me1 and H4K20me2 peptides, although not as robustly as observed on core histones (Suppl Fig. S2c), indicating that histone peptides are not as effective as core histones for LSD1n as substrates. In addition, we found that both LSD1c and LSD1n interact with histone H3 or H4 tails *in vitro* (Suppl Fig. S3a, S3b), while CoREST interacts with H4 tail (Suppl Fig. S3c). We further mapped the CoREST-H4 interaction region to the N-terminal ELM2 domain of CoREST (Suppl Fig. S3d, S3e), which has been identified in many chromatin-associated proteins while its function is largely unknown. These observations suggest that CoREST enhances LSD1n enzymatic activity through direct interaction with histone H4. Because LSD1n can demethylate H4K20 on a truncated histone H4 peptide (H4 aa10–30), we speculate that it may adopt a different conformation compared to the previously reported structure of LSD1n/CoREST complex with the N-terminal of histone H3 tail[11]. Novel conformations of LSD1 have been suggested when LSD1 removes methylation on non-histone substrates such as p53[12].

The finding that the purified LSD1n was incapable of H3K4 or H3K9 demethylation is in agreement with the recent report that LSD1n can mediate H3K9me2 demethylation only in association with Supervilin-containing complex in differentiated neuronal cell lines[13]. These results emphasize the importance of uncovering the global genomic distribution of the distinct LSD1 isoforms in neurons.

LSD1 occupies gene promoters and enhancers

LSD1 has been previously reported to regulate gene expression by occupying active gene promoters and enhancers[9, 14], and to function as an enhancer "decommissioner" during embryonic stem cell differentiation[14]. However, its roles in differentiated neurons remain relatively unexplored. In order to identify which genes were direct targets of LSD1c or LSD1n, genome-wide mapping experiments by chromatin immuno-precipitation coupled with deep sequencing (ChIP-seq) were performed in mouse cortical neurons using an antibody that recognizes total LSD1. Using a standard KCl-mediated depolarization protocol to mimic neuronal activity stimulation[15], we identified 11,218 and 12,701 LSD1-binding sites in primary cortical neurons in resting and active states respectively, of which 5471 were common binding sites under both conditions (Fig. 1c). LSD1 binding sites were enriched on gene promoters and enhancers, consistent with previously published LSD1 genome-wide localization analyses[9, 14]. To distinguish LSD1n from LSD1c, we generated *LSD1c* and *LSD1n* transgenic mice, which express FLAG-tagged isoform-specific *LSD1* upon tamoxifen-induced Cre-mediated recombination (Suppl Fig. S4a). The expression level of the transgenic LSD1 isoforms was similar to the endogenous level (Suppl Fig. S4b). We observed similar genome-localization of LSD1c and LSD1n in ChIP-seq experiments using anti-FLAG antibody to specifically detect each isoform, indicating that the recruitment of LSD1 was not isoform-specific (Fig. 1d and Suppl Fig. S4c, S4d). Interestingly, we observed decreased level of H4K20me1 on signal-dependent LSD1-binding sites at promoters and enhancers after KCl-mediated depolarization (Fig. 1d, 1e), without significant changes of other histone marks, except a slightly increased level of H3K4me1 on those LSD1-binding promoters, based on meta-analysis of ChIP-seq experiments (Fig. 1e). These data suggest that the recruitment of LSD1 correlates with specific removal of H4K20 methylation in a genome-wide fashion. In addition, we observed that neurons over-expressing *LSD1n* exhibited decreased global level of H4K20 methylation (Suppl Fig. S4e), consistent with the observation of LSD1n-dependent H4K20 demethylation activity *in vitro*.

To explore which transcription factors might recruit LSD1 to these sites, we performed *de novo* sequence motif analyses using the HOMER software package[16]. We found that CTCF or CTCF-like Boris recognition motifs were specifically enriched in enhancer sites where LSD1 occupancy was lost after KCl-mediated depolarization (Suppl Fig. S4f). Conversely, MEF2 binding motifs were specifically enriched in LSD1-bound enhancer sites gained after depolarization (Suppl Fig. S4g), while CREB binding motifs were specifically enriched in gained LSD1-bound promoter sites (Suppl Fig. S4h). This result suggests that LSD1 may target enhancer and promoter elements regulated by transcription factors MEF2 and CREB, which are known to be crucial for neuronal activity-regulated gene transcription[17]. Indeed, immuno-precipitation assays revealed that LSD1 could form a complex with both MEF2 and CREB (Suppl Fig. S4i), supporting the idea that LSD1 might function as a co-regulator of

these transcription factors. Furthermore, genome-wide mapping of MEF2 by ChIP-seq confirmed that both LSD1 and MEF2 occupy a subset of neuronal enhancers (Suppl Fig. S4j, S4k, S4l)[17]. Specifically, 4482 of 5320 (84%) gained LSD1-occupied enhancers were also bound by MEF2 (Suppl Fig. S4j), suggesting that MEF2 might recruit LSD1 to these enhancer sites. Consistent with this prediction, depolarization-induced recruitment of LSD1 was observed on known enhancer elements regulated by MEF2, including those in *Npas4*, *Arc* and *Egr1* loci (Fig. 1f and Suppl Fig. S4m, S4n). These data suggest a regulatory role of LSD1 on the neuronal activity-regulated genes.

LSD1n controls neuronal activity-regulated gene expression

To investigate the *in vivo* role of LSD1n in transcriptional control, we initially performed global transcriptional profiling analysis by RNA-seq using a conditional knockout model of LSD1, which deleted both *LSD1c* and *LSD1n* upon Cre-mediated recombination[10]. Primary cortical neurons were cultured for 10 days *in vitro* before KCl-mediated depolarization (6 hours). We found that KCl-induced gene transcription was largely compromised in cortical neurons following *LSD1* deletion (Suppl Fig. S5a), providing initial evidence that LSD1 is involved in the regulation of neuronal activity-regulated gene transcription. To assess the extent by which LSD1n contributes to this regulatory mechanism, we generated a conditional knockout mouse model targeting *LSD1n* (Fig. 2a). Upon Nestin-Cre mediated recombination, the *LSD1n* conditional knockout mice express *LSD1c* only, while WT control mice express *LSD1n* as the dominant form in cortical neurons (Suppl Fig. S5b), and the total level of LSD1 appeared to be unchanged (Suppl Fig. S5b, S5c). By using this strategy, we performed global transcriptional profiling experiments by RNA-seq in cortical neurons isolated from E15.5 embryos of *LSD1n* knockout or WT control. RNA-seq analysis revealed that 454 genes were up-regulated following 6 hours of KCl-mediated depolarization in WT neurons (Suppl Fig. S5d), and that *LSD1n*-deficient cortical neurons exhibited an impaired transcriptional response (Suppl Fig. S5d), suggesting that LSD1n was indispensable for the neuronal activity-regulated gene expression. To determine whether LSD1n regulates gene expression at the transcriptional or post-transcriptional level, we performed global run-on coupled with deep-sequencing analysis (GRO-seq)[18], which enabled us to directly measure transcriptional events. Analysis of the GRO-seq experiments revealed that 1548 genes were up-regulated 1 hour of KCl-mediate depolarization in WT control neurons (Fig. 2b, 2c). The transcriptional response was significantly impaired in *LSD1n*-deficient cortical neurons (Fig. 2b, 2c). For example, transcription of *Npas4*, encoding a critical neuronal activity-regulated transcription factor[19], was up-regulated upon KCl treatment in WT neurons, while its activation was compromised in *LSD1n*-deficient neurons (Fig. 2d). Similar results were observed for other neuronal activity-regulated genes, such as *Arc* and *Egr1* (Suppl Fig. S5e, S5f), and were validated by RT-qPCR (Fig. 2e). It has been reported that some of neuronal activity-regulated enhancers express non-coding RNAs, called eRNAs[15, 20]. We found that expression of KCl-induced eRNAs, such as eRNAs from enhancers of *Arc*, *Fos*, *Npas4* and *Nr4a1* loci (Suppl Fig. S5g), are decreased in *LSD1n*-deficient neurons measured by RT-qPCR (Suppl Fig. S5h), suggesting a regulatory role of LSD1n on enhancer activity. In addition, LSD1n is bound to the promoters of the majority of neuronal activity-regulated genes, as shown by LSD1n ChIP-

seq (Suppl Fig. S5i), suggesting that LSD1n regulates gene expression of its target genes acting on binding to both gene promoters and enhancers.

LSD1n removes histone H4 K20 methylation *in vivo*

To determine the causality between LSD1n-dependent transcriptional changes and histone demethylation, we performed H3K4me1, H3K9me2, H3K36me3 and H4K20me1 ChIP-seq experiments using WT or *LSD1n* deficient neurons. While the levels of H3K4me1, H3K9me2 or H3K36me3 were not significantly changed on LSD1-binding sites at promoters or enhancers in *LSD1n* deficient cortical neurons based on meta-analysis of ChIP-seq experiments (Suppl Fig. S6a, S6b, S6c), the H4K20 methylation levels were significantly increased on LSD1-bound promoters and enhancers in a genome-wide fashion (Suppl Fig. S6d). This is consistent with our initial result showing that LSD1n can function *in vitro* as a H4K20 demethylase (Fig. 1b). Furthermore, we observed no signification changes or slight decrease of other histone methylation markers including H3K4me2, H3K9me2 and H3K79me2 on promoters of LSD1n gene targets, including *Naps4* and *Arc* (Suppl Fig. S6e, S6f, S6g), consistent with our hypothesis that LSD1n specifically targets H4K20me1 but not other methylated histone substrates. Further analysis of H4K20me1ChIP-seq revealed that this histone mark was significantly increased on transcribed coding regions of neuronal activity-regulated genes (Fig. 3a) that are *LSD1n*-dependent (Fig. 2b, 2c), consistent with a repressive role of H4K20me1 on gene expression. Supporting the idea of a direct effect of *LSD1n* deletion on H4K20 methylation, we observe that the global H4K20 methylation levels are increased in *LSD1n* deficient neurons (Suppl Fig. S6h), but reduced in *LSD1n* over-expressing neurons (Suppl Fig. S4e). These results strongly support our finding that LSD1n can remove the H4K20 methylation mark *in vivo*. Furthermore, the expression level of known H4K20 methyltransferases (*Pr-Set7/Setd8*, *Suv420h1*, *Suv420h2*) [21, 22] and demethylases (*Phf8*, *Phf2*) [23–25] is not significantly changed in *LSD1n* deficient neurons (based on RNA-seq and GRO-seq experiments), except for a slight increase of *PHF8* proteins (Suppl Fig. S6h), supporting our conclusion of a direct role of LSD1n as a H4K20 demethylase in cortical neurons. Furthermore, we noticed that the expression level of *Phf8* was low in cortical neurons where *LSD1n* was abundant (Suppl Fig. S6i). Consistent with these data, shRNA-mediated down-regulation of *Phf8* did not alter the KCl-induced transcriptional response of LSD1n target genes (Suppl Fig. S6j, S6k), suggesting that LSD1n, but not PHF8, mediates the H4K20 demethylation events in response to neuronal activity *in vivo*.

We investigated the possibility that LSD1n may utilize both H3K9 and H4K20 methylated substrates to activate gene expression in cortical neurons, which is particularly intriguing based on the finding that LSD1n can mediate H3K9me2 demethylation in association with Supervilin-containing complex[13] that occurs during differentiation protocols. However, we do not observe significant changes of H3K9me2 levels on LSD1n-binding sites at promoters or enhancers in cortical neurons (Suppl Fig. S6b, S6f). Instead, we find increased H4K20me1 levels on those targets (Fig. 3a and Suppl Fig. S6d). Because Svil expression is reported to be transiently induced upon neuronal differentiation in a human neuroblastoma cell line[13], we determined the expression level of *Svil* in mouse cortical neurons. Surprisingly, using validated primer sets and RNA-seq results, *Svil* expression was found to

be extremely low in cortical neurons compared to the levels of *LSD1* (Suppl Fig. S6i), suggesting that Svil-dependent H3K9 demethylation may not play a role in LSD1n-dependent transcriptional control in cortical neurons.

LSD1n promotes transcriptional initiation and elongation

The finding that H4K20me1 levels were high across transcribed coding regions, consistent with a previous report[26], suggested that LSD1n might regulate elongation. To test this hypothesis, we performed RNA polymerase II (Pol II) ChIP-seq experiments using WT control or *LSD1n* deficient neurons. Analysis of RNA Pol II genome-wide distribution revealed that KCl-mediated depolarization leads to an induction of both transcriptional elongation and initiation steps, as shown by the increased RNA Pol II signals on the transcription start sites (TSS) and transcribed coding regions of neuronal activity-regulated genes, including *Npas4* (Fig. 3b), *Arc* and *Egr1* (Suppl Fig. S7a, S7b). To examine the global effect of LSD1n on elongation, we calculated the RNA Pol II traveling ratio (TR) of neuronal activity-regulated genes, based on RNA Pol II ChIP-seq experiments, which revealed a statistically significant shift of RNA Pol II signals (increased pausing) in *LSD1n* deficient neurons compared to WT controls (Fig. 3c, 3d), supporting the hypothesis that LSD1n is involved in regulation of elongation in a genome-wide fashion. These results were further confirmed by the analysis of the traveling ratio based on GRO-seq experiments by comparing WT and *LSD1n* deficient neurons after KCl-mediated depolarization (Suppl Fig. S7c). To further validate the roles of LSD1n on transcription initiation and/or elongation steps, we analyzed the RNA Pol II binding on the TSS and across the transcribed coding regions of KCl depolarization-induced transcription units, including *Arc*, *Egr1* and *Npas4*. Because RNA Pol II density over transcribed coding regions was dependent on initiation and elongation steps, the RNA Pol II density ratio between the 3′ region (coding region) and the 5′ region (TSS) can serve as a surrogate index for RNA Pol II pause-release status. In this analysis, higher values indicate increased release, and lower values indicate increased pausing. One hour after KCl-mediated depolarization, the RNA Pol II intensity on *Npas4* TSS (measured by 5′ PCR probe) was significantly increased in WT neurons, but this effect was compromised in *LSD1n* deficient neurons (Fig. 3e), suggesting that the transcription initiation of *Npas4* gene was compromised in the *LSD1n* deficient neurons. Simultaneously, the RNA Pol II density across the *Npas4* coding region (measured by 3′ PCR probe) was increased in WT neurons after KCl treatment, but was compromised in *LSD1n* deficient neurons (Fig. 3f). Furthermore, we observed that in WT control neurons, the RNA Pol II 3′/5′ ratio for *Npas4* gene was increased after treatment, indicating that KCl-mediated depolarization had a greater effect on the elongation step compared to the initiation step; this effect was reduced in the *LSD1n* deficient neurons, indicating a role of LSD1n in transcriptional elongation control (Fig. 3g). Similarly, transcription elongation of *Arc* and *Egr1* were also compromised in *LSD1n* deficient neurons, as measured by RNA Pol II ChIP (Suppl Fig. S7d–S7i).

Our findings are consistent with a previous report demonstrating that *Arc* gene expression is regulated by promoter-proximal RNA polymerase II stalling upon neuronal activity stimulation[27]. We confirmed this previous observation in our genome-wide analysis (Fig. 3d and Suppl Fig. S7j). Here, we provide evidence that this mechanism is LSD1n-dependent

(Fig. 3c, 3d and Suppl Fig. S7c). A similar promoter-proximal RNA Pol II pause/release regulation has also been reported for genes induced upon TLR4-mediated gene activation[28], suggesting that elongation control plays an important role in signal-dependent trancription[29].

Because H4K20me1 has been reported to inhibit CBP/p300 histone acetyltransferase activity toward H4K16Ac *in vitro*[21], we examined whether the increased level of H4K20me1 observed in *LSD1n* deficient neurons might affect H4K16Ac *in vivo*. We found decreased levels of H4K16Ac on promoters of *LSD1n* target genes, such as *Npas4* and *Arc* (Suppl Fig. S7k). This observation correlates with the increased levels of L3MBTL1 (Suppl Fig. S7l), an H4K20me1 reader[30], and the decreased recruitment of Brd4 (Suppl Fig. S7m), a reader of histone acetylation and a critical regulator of transcriptional elongation[31], on LSD1n binding sites. Together these results imply that H4K20me1 may prevent Brd4 recruitment by affecting H4K16 acetylation and/or recruitment of repressive L3MBTL1, hence inhibiting transcriptional elongation. Consistent with the results based on RNA Pol II ChIP-seq experiments, we found that the levels of H3K36me3, a histone marker associated with elongation[26], were decreased on transcribed coding regions of neuronal activity-regulated genes in *LSD1n* KO neurons (Fig. 3h), but not on LSD1-binding sites at promoters or enhancers (Suppl Fig. S6c), indicating that *LSD1n* deficiency causes a defect in transcriptional elongation of neuronal activity-regulated genes. In addition, we observed increased recruitment of LSD1n on the transcribed coding regions of neuronal activity-regulated genes after KCl-mediated depolarization (Suppl Fig. S7n, S7o, S7p), suggesting that LSD1n promotes neuronal activity-regulated transcriptional elongation by removing H4K20 methylation in transcribed coding regions.

LSD1n is required for spatial learning and memory

Because LSD1n is required for regulated gene expression induced by neuronal activity, which regulates its genomic localization, we hypothesize that LSD1n might play a critical role in learning and memory. Therefore, we analyzed the behavioral phenotype of the brain-specific *LSD1n* knockout mice (*LSD1n NesCre*). *LSD1n* knockout mice can survive to adulthood and show no obvious anatomical abnormality (Suppl Fig. S8a). In addition, *LSD1n* deficient mice show normal activity in the optomotor and locomotor activity tests (Suppl Fig. S8b, S8e), indicating that *LSD1n* deficient mice have normal vision and movement abilities, permitting the behavioral assessment experiments to determine the roles of LSD1n in learning and memory. To this aim, we used a set of standard behavioral tasks assessing spatial learning and memory, which have been previously linked to mechanisms of neuronal activity-regulated gene transcription[32]. While *LSD1n* knockout mice did not show any impairment in the Y Maze Spontaneous Alternation test, which measures simple working memory (Suppl Fig. S8c, S8d), we observed cognitive deficits when the Barnes maze test was performed using sex- and age-matched WT control and *LSD1n* knockout mice (Fig. 4a). While WT control mice identified the target quadrant relative to the other non-target quadrants of the maze, *LSD1n* knockout mice failed to identify the target after training (Fig. 4a), indicating that *LSD1n* knockout mice exhibited impaired spatial learning. In addition, *LSD1n* knockout mice showed significant impairments in performing the novel object recognition task. Indeed, *LSD1n* knockout mice failed to distinguish novel objects from familiar objects in this behavioral paradigm (Fig. 4b, 4c), indicating that *LSD1n* was

required for recognition memory. While it has been reported that *LSD1* plays an important role in circadian rhythmicity[33], *LSD1n* knockout mice appeared to have normal motor activities when tested in dark and light cycles (Suppl Fig. S8e), suggesting that *LSD1n* is not required for this behavior.

In order to examine the extent of which LSD1n-dependent transcriptional regulation was correlated to the defects in learning and memory, we measured the expression level of neuronal activity-regulated genes, including *Arc*, *Btg2*, *Egr1* and *Npas4.* We observed that the expression of those genes was decreased in *LSD1n* knockout mice compared to their WT littermate controls (Fig. 4d). Additionally, *LSD1n* knockout mice exhibited increased levels of H4K20 methylation (Suppl Fig. S8f), consistent with our observations that LSD1n plays an active role as a histone H4K20 mono- and di- methyl demethylase in cortical neurons (Suppl Fig. 6h).

It has been documented for more than forty years that histone H4K20 methylation level increased in aged rat brain[34], and that histone H4K20me3 level increased in quiescence and senescence[35]. Here, we find that *LSD1n* level was decreased, while total level of *LSD1* transcript was almost unchanged, in aged mice (Suppl Fig. S8g, S8h). It will be interesting to determine whether the decreased expression of *LSD1n* contributes to the age-related H4K20me level increases and cognitive impairments, such as memory loss.

Taken together, we found that an alternative splicing event occurring only in neurons switches the enzymatic demethylase activity of LSD1 from histone H3K4 to histone H4K20 methylated substrates in post-mitotic cortical neurons, and that this unique isoform of LSD1 promotes neuronal activity-regulated gene expression, facilitating both transcription initiation and elongation steps. This has proven to be essential for spatial learning and long-term memory formation (Suppl Fig. S9).

Discussion

Because LSD1n can mediate H3K9me2 demethylation in association with Supervilin-containing complex during neuronal differentiation events[13], it is possible that both H3K9 and H4K20 demethylase activities of LSD1n contribute to its brain functions. Interestingly, it has been reported that the deficiency of G9a/Glp, the major H3K9 methyltransferases for H3K9me2, can induce de-repression of a subset of genes involved in neuronal differentiation[36,37]. Thus, it is likely that LSD1n-dependent H4K20 demethylation is linked to transcriptional events essential for learning and memory, while its H3K9 demethylase function is required for gene expression during neuronal differentiation.

Although CoREST enhances LSD1n-dependent H4K20 demethylation *in vitro*, *CoREST/Rcor1* is not required for LSD1n function in neurons since *CoREST/Rcor1* knockout mice have normal brain functions (personal communications with Dr. Gail Mandel). However, *Rcor1/Rcor2* double knockout mice are embryonic lethal, revealing similar phenotype with total *LSD1* knockout mice (Our unpublished data and personal communications with Dr. Gail Mandel). It is possible that *Rcor2*, a homologue of *CoREST/Rcor1*, can compensate functions of *CoREST in vivo*. It is interesting that CoREST complex contains both

HDAC1/2 and LSD1, while HDAC1/2 and LSD1 have distinct function in neuronal gene expression regulation. It will be an interesting topic to investigate in the future.

Because LSD1 is not only located at promoters and transcribed coding regions, but high enrichment is also observed at enhancers elements, we cannot exclude that LSD1-bound enhancers play a role in regulating neuronal gene expression (Suppl Fig. S5i, S7n, S7o, S7p). It is possible that promoter-enhancer looping may act as a mechanism to deliver LSD1n from distal enhancers to promoters and transcribed coding regions to remove negative H4K20me1 mark. eRNAs expression could also contribute to neuronal activity-dependent gene expression as recently reported[20,40], and we hypothesize that LSD1n may regulate eRNA expression in a fashion mechanistically similar to the regulation of protein-coding genes, enhancing transcription elongation by facilitating H4K16 acetylation and Brd4 recruitment, and/or inhibiting L_3MBTL1 recruitment

H4K20 methylation is the major lysine methylation site on histone H4, and is involved in cell cycle regulation, DNA damage response, mitotic chromatin condensation and transcription regulation[38]. However, the effect of H4K20me1 on transcriptional control and brain function is poorly understood. Our data suggest that H4K20me1 serves as a negative regulator of gene expression/elongation, which is signal-dependent, and is associated with neuronal-specific events. PHF8 deficiency has been linked to mental retardation[39]; however it is not clear whether the defects observed are due to cell cycle regulatory functions of PHF8. The characterization of LSD1n reveals the important role of H4K20 methylation on transcription elongation control and cognitive functions such as spatial learning and memory.

One cannot help but speculate about why this unique alternative splicing event of LSD1 occurs specifically in neurons. There are at least two non-mutually exclusive possibilities. It could be that neurons require this novel demethylase to maintain proper H4K20 methylation level since they have lost the ability to reset H4K20 methylation state by cell cycle-dependent histone mark deposition, which would appropriately methylate newly incorporated histones. The other possible explanation is that H4K20 methylation serves as a novel marker to regulate transcription in neurons because its role during cell cycle has been relieved. Neurons might have acquired this enzymatically-unique isoform to remove H4K20me1/2 and achieve more precise control of gene expression in complex processes such as learning and memory.

Materials and Methods

Generation of conditional knockout mice of *LSD1n* and transgenic mice

The conditional knockout mice of *LSD1n* were generated by targeted mutagenesis in embryonic stem cells to insert two LoxP sites using pLNL vector provided by Dr. Ju Chen (UC San Diego), flanking exon 8a of *LSD1*. Correct targeting was established by Southern blots with 5′ and 3′ external probes and PCR. The Neo-cassette was removed by using *flpase* mice. *FLAG-LSD1c* and *FLAG-LSD1n* transgenic mice were generated by targeted mutagenesis in embryonic stem cells to insert pCAG-LSL-FLAG-LSD1c or pCAG-LSL-FLAG-LSD1n into *Rosa26* locus using pCAG-LSL vector provided by Dr. Sen Wu and

Mario Capecchi (U of Utah). Correct targeting was established by PCR. Embryos were genotyped using PCR. All mice were maintained according to standard animal protocols approved by UC San Diego. The histological analysis by Nissl staining was performed to analyze brain anatomy and was successfully repeated one time.

Antibodies

LSD1 ab17721, Histone H4 ab31830, H4K20me1 ab9051, H4K20me2 ab9052, H3K79me2 ab3594, L3MBTL1 ab51880, H3K9me2 ab1220, H3K4me1 ab8895 and GST ab9085 (Abacm); ANTI-FLAG M2 Affinity Gel (A2220) (Sigma); H4K16Ac 39167 (Active Motif); H3K4me2 07-030, H3K36me3 07-549, CoREST 07-455 and CREB 17-600 (Millipore); Brd4 A301-985A (Bethyl Laboratories); H4 sc-10810, H3 sc-8654 and MEF2 sc-313, RNA Pol II sc-899 and His-probe sc-803 (Santa Cruz Biotechnology); histone H3 #9715 and H3K27me2 #9755 (Cell Signaling Technology)

Generation of recombinant proteins, *in vitro* demethylase assay and histone peptide array

Recombinant LSD1 proteins with N-terminal His6 tag and C-terminal FLAG tag were bacterially expressed and purified using a two-step affinity purification approach: Ni-NTA affinity chromatography followed by M2-anti-FLAG affinity purification. The purified proteins were desalted after FLAG-peptide elution. Recombinant CoREST proteins with a N-terminal GST tag and a terminal HIS6 tag were purified using a similar strategy. Histone demethylase assays were performed as previously described[7]. Briefly, core histones, nucleosomes or histone peptides were incubated with purified recombinant proteins in the histone demethylase activity (HDM) assay buffer (50mM TrisHCl pH 8.5, 50mM KCl, 5mM $MgCl_2$, 0.5% BSA, and 5% glycerol) from 1 to 4 hours at 37°C. The reaction mixture was analyzed by SDS-PAGE/Western blots using specific antibodies, or by MALDI-TOF mass spectrometry to identify the demethylated peptides. The histone demethylase experiments were successfully repeated one time. The histone peptide binding assay was successfully performed one time using the MODified Histone Peptide Array (#13005, Active Motif) following the manufacturer's instructions.

Cortical neuronal culture and membrane depolarization by potassium chloride (KCl)

Cortical neurons were prepared as previously described[15]. Briefly, E15.5 mouse embryo cortices were dissected and then dissociated in 1× Hank's Balanced Salt Solution (HBSS) in the presence of 0.1% trypsin (Invitrogen). Trypsin treatment was terminated with trypsin inhibitor and triturated in presence of DNase I (Sigma). Neurons were pooled after genotyping and seeded on poly-D-lysine coated dishes. Neurons were maintained in Neurobasal medium containing B27 supplement, antibiotics and glutamine. Neurons were cultured *in vitro* for 10 days. One third of the medium was replaced with fresh warm medium every two days.

For KCl depolarization, neurons were quieted overnight in 1 μM tetrodotoxin (TTX, Tocris), and then were incubated for 0, 1, 3, 4 or 6 hours in 55 mM KCl as described previously[15]. ChIP-seq experiments were performed after 0 or 1 h KCl-mediated depolarization. RNA-seq experiments were performed after 0 or 6 hours KCl-mediated depolarization. GRO-seq experiments were performed after 0, 1 or 3 hours KCl-mediated depolarization. 3X

depolarization buffer (170mM KCl, 1mM $MgCl_2$, 2 mM $CaCl_2$, 10mM HEPES pH=7.9) was added as 1:3 ratio into culture medium (final 55mM KCl) to induce depolarization of cortical neurons.

Total protein extracts and immunoprecipitation

Primary neurons were collected in cold PBS. Brain cortical dissections were homogenized in cold PBS. Samples were lysed with lysis buffer (20mM Tris pH 7.4, 150mM NaCl, 1mM EDTA, 1% IGEPAL, protease inhibitor cocktail). For immunoprecipitation assay, 1mg of total lysate was incubated overnight at 4°C with 2ug of specific antibody. The day after the antibody-protein complexes were bound to protein G dynabeads (Thermo Fisher) and then washed 3 times with lysis buffer and boiled for Western blots analysis. Western blots were successfully repeated one time.

ChIP, ChIP-seq, RNA-seq and GRO-seq

Chromatin Immuno-precipitation (ChIP) assays were performed according to the previously described protocol[14]. For all ChIP-seq experiments, cortical neurons were harvested after crosslinking in presence of 1% formaldehyde for 10 minutes with the exception of LSD1, FLAG-LSD1c or FLAG-LSD1n ChIP-seq experiments, in which cortical neurons were cross-linked using 2mM disuccinimidyl glutarate (DSG) (ProteoChem c1104-100mg) for 45 minutes before formaldehyde treatment. ChIP experiments were performed using the specific antibodies.

ChIP libraries were prepared as previously described[40]. RNA-seq experiments were performed as previously described[41]. GRO-seq experiments were performed as previously described[18]. The sequencing experiments were successfully repeated one time.

Behavioral studies

Behavioral studies were conducted at The Scripps Research Institute (TSRI) Mouse Behavioral Assessment Core according to approved animal protocols. The behavioral assessments were performed as previously reported[42–47]. Ten pairs of age- (2-month-old) and sex-matched (20 male and 20 females) WT control or *LSD1n* KO mice (C57Bl/6 background) were used in all the behavioral assessment experiments. Mouse behavioral specialists blind to the genotype scored all parameters. Locomotor activity was measured for 24 hours in polycarbonate cages placed into frames mounted with two levels of photocell beams at 2 and 7 cm above the bottom of the cage (San Diego Instruments, San Diego, CA). Vision was assessed by counting head tracks made by mice on a stationary elevated platform surrounded by a rotating drum with black and white striped walls. Simple working memory and exploration was measured in the Y maze test[45]. Spatial learning and memory were examined in the Barnes maze essentially as described[46, 47]. Four sequential daily acquisition sessions were performed using a maze containing 20 holes, where mice were trained to identify the correct hole and enter the escape tunnel below. Subsequently, memory was assessed in the probe test in which the escape tunnel was removed and the mice were free to explore the maze for 3 minutes. The time spent in each quadrant was determined and the percent time spent in the target quadrant (the one originally containing the escape box) was compared with the average percent time in the other three quadrants. A two trial novel

object recognition test was used in which the mice were exposed to 2 identical objects in a rectangular arena on day 1. 24 hour later the mice were returned to the arena with one of the same objects (familiar) as well of a new object (novel) in the same locations as the previous day. Contacts made with the objects in the second 5 min test were used to determine if the mice recognized novelty by exploring the novel object more than the familiar object during this trial.

RT-qPCR, ChIP-qPCR

Total RNAs were isolated from cultured cortical neurons or dissected brain tissues using Qiagen RNeasy Mini Kit according to the standard protocol. cDNA was synthesized using Invitrogen Superscript III cDNA synthesis kit according to manufacturer's protocol. Real time PCR (qPCR) was performed by standard SYBRGreen™ protocol using a Stratagene Mx3000 machine. For normalization, expression levels were calculated relative to the levels of *Actb* transcripts. ChIP-qPCR experiments were performed according to the previously described protocol[14]. Experiments involving WT or LSD1-KO mice were performed after pooling cortices from 8 to 12 individual embryos and qPCR experiments were repeated 3 to 4 times as reported in the Reporting Checklist and figure legends, and one representative result was shown in the figures. shRNA experiments were performed from 3 independent replicates. P-values were calculated using an unpaired t-test. Primer sets were listed in the supplemental method section.

ChIP-seq analysis and *de novo* motif discovery

ChIP-seq peak identification, quality control, and motif analysis were performed using HOMER (http://biowhat.ucsd.edu/homer) as described[16]. Genome binding peaks for LSD1 were identified using the 'findPeaks' command in HOMER with setting of '–style factor': 500 bp peaks with 4- fold enrichment and 0.001 FDR significance over local tags, and normalization to 10 million mapped tags per experiment. Peaks from separate experiments were considered co-bound if their peak centers were located within 1kb region of each other. For de novo motif analysis, transcription factor motif finding was performed on +/−500 bp relative to the peak center defined from ChIP-seq. Peak sequences were compared to random genomic fragments of the same size and normalized G/C content to identify motifs enriched in the ChIP-seq targeted sequence. To generate histograms for the average distribution of tag densities, position-corrected, normalized tags in 50 bp windows were tabulated within the indicated distance from specific sites in the genome. Clustering plots for normalized tag densities at each genomic region were generated using HOMER and then clustered using Cluster (http://bonsai.hgc.jp/~mdehoon/software/cluster/software.htm/) and visualized using Java TreeView, as described[48].

To determine LSD1-binding active enhancers, putative enhancers sites were first defined based on ChIP-seq enrichment of H3K4me1 flanking −/+ 1,000 bp from the center of the LSD1 peaks. Putative enhancers were defined by the following criteria: (1) regions were at least 3 kb away from annotated TSSs; (2) regions had at least 16 tags from H3K4me1 ChIP-seq normalized to 10 million tags; and (3) regions had at least 10 tags from GRO-seq normalized to 10 million tags.

Genome-wide gene expression analysis with GRO-seq

GRO-seq analysis of genome-wide gene expression was performed by HOMER followed by edgeR[16, 49]. Briefly, HOMER was used to generate a gene expression matrix by identifying uniquely mapped RNA tags to gene body that is from 500bp downstream of TSS to 13kb the annotated end if gene body is shorter than 13kb, based on RefSeq annotation for the mouse genome (mm9). Statistical analysis for differential expression was performed using edgeR on raw sequencing reads from neurons that were treated with or without KCl. To identify the different expressed genes that were governed by *LSD1n*, cultured cortical neurons were incubated for 0, 1, 3h and then were used for GRO-seq experiments. All six GRO-seqs were normalized to 10 million tags, and HOMER was used to quantify gene expression by tabulating normalized RPKM value for the gene body of each gene. Genes with a >1.5-fold change in GRO-seq signal was considered to be differentially expressed.

Traveling Ratio (TR) Calculation

TR calculation was performed as described[50]. TR was defined as the relative ratio of RNA Pol II density in the promoter-proximal region and the gene body. The promoter proximal region refers to the window from −50bp to +300bp surrounding transcription start site (TSS). The significance of the change of TR between wild type and *LSD1n* knockout samples was calculated using two-tailed Kolmogorov–Smirnov (KS) test.

Statistics

No statistical methods were used to pre-determine sample sizes but our sample sizes are similar to those generally employed in the field. No randomization and blinding were employed. Data distribution was assumed to be normal but this was not formally tested. There was correction for multiple comparisons. No animals or data points were excluded from analyses.

The p value, degree of freedom and t value are calculated using on-line tools from http://www.graphpad.com/quickcalcs/ttest1.cfm. The exact p-values are reported in the figure legends; the degree of freedom T, D and F values are calculated as follow:

Fig. 2b (t(3094)=10.9466 (WT 0hr vs KO 0hr); t(3094)=19.8081 (WT 1hr vs KO 1hr)); Fig. 2e (t(4)=24.9433 (Arc); t(4)=31.5490 (Btg2); t(4)=9.4574 (Cyr61); t(4)=54.8099 (Egr3); t(4)=16.0747 (Npas4); t(4)=13.5977 (Pcsk1)); Fig. 3c (D = 0.0879 (WT +KCl vs KO +KCl)); Fig. 3d (t(3094)=11.1432 (WT 0hr vs KO 0hr); t(3094)=14.2081 (WT 1hr vs KO 1hr)); Fig. 3e (t=20.944 (WT KCl− vs WT KCl+); t=9.5021 (WT KCl+ vs KO KCl+)); Fig. 3f (t=19.9576 (WT KCl− vs WT KCl+); t=12.1616 (WT KCl+ vs KO KCl+)); Fig. 3g (t=15.4007 (WT KCl− vs WT KCl+); t=7.5804 (WT KCl+ vs KO KCl+)); Fig. 4a (F(18)=4.978 (WT); F(18)=0.791 (KO)); Fig. 4b (F(18)=14.273 (WT); F(18)=1.052 (KO)); Fig. 4c (F(18)=11.804 (WT); F(18)=0.068 (KO)); Fig. 4d (t(6)=4.1380 (Arc); t(6)=4.5364 (Btg2); t(6)=2.9203 (Egr1); t(6)=3.6844 (Junb); t(6)=2.5411 (Npas4); t(6)=6.2686 (Nr4a1)); Fig. S5a (t(944)=0.7348 (WT −KCl vs KO −KCl); t(944)=4.8120 (WT +KCl vs KO +KCl)); Fig. S5b (t(4)=0.2669 (LSD1); t(4)=4.4133 (LSD1n)); Fig. S5d (t(906)=1.7757 (WT −KCl vs KO −KCl); t(944)=8.6811 (WT +KCl vs KO +KCl)); Fig. S5h (t(6)=5.7958 (Arc eRNA−KCl+); t(6)=3.182 (Arc eRNA+ KCl+); t(6)=3.501 (Fos eRNA-KCl+); t(6)=3.705 (Fos

eRNA+ KCl+); t(6)=8.745 (Npas4 eRNA+ KCl+); t(6)=3.852 (Nr4a1 eRNA− KCl+)); Fig. S6e (t(6)=0.1253 (Npas4); t(6)=0.7265 (Arc)); Fig. S6f (t(6)=1.2827 (Npas4); t(6)=3.1955 (Arc)); Fig. S6g (t(6)=0.9850 (Npas4); t(6)=3.4472 (Arc)); Fig. S6j (t (4) = 5.0265 (shC KCl − vs shPhf8 KCl-) t (4) = 5.5407 (shC KCl+ vs shPhf8 KCl+)); Fig. S6k (t(4) = 0.8241(Arc); t(4) = 1.0072 (Btg2); t (4)= 1.5791(Cyr61); t (4)= 0.9688 (Egr3); t (4) = 1.2397 (Npas4); t (4)= 1.0180 (Psck1)); Fig. 7c (D = 0.1063 (WT +KCl vs KO +KCl)); Fig. 7d (t(6)=4.9448 (WT KCl− vs WT KCl+); t(6)=2.3124 (WT KCl+ vs KO KCl+)); Fig. 7e (t(6)=7.6956 (WT KCl− vs WT KCl+); t(6)=5.2179 (WT KCl+ vs KO KCl+)); Fig. 7f (t(6)=5.2133 (WT KCl− vs WT KCl+); t(6)=6.2577 (WT KCl+ vs KO KCl+)); Fig. 7g (t(6)=7.4153 (WT KCl− vs WT KCl+); t(6)=4.3140 (WT KCl+ vs KO KCl+)); Fig. 7h (t(6)=37.8704 (WT KCl− vs WT KCl+); t(6)=24.5796 (WT KCl+ vs KO KCl+)); Fig. 7i (t(6)=7.7317 (WT KCl− vs WT KCl+); t(6)=4.6164 (WT KCl+ vs KO KCl+)); Fig. 7j (D = 0.1545 (−KCl vs +KCl)); Fig. 7k (t(6)=2.6156 (Npas4); t(6)=4.1147 (Arc)); Fig. 7k (t(6)=2.6156 (Npas4); t(6)=4.1147 (Arc)); Fig. 7l (t(4)=7.2086 (Npas4);t(4)=5.1777 (Arc)); Fig. 7m (t(4)=7.5372 (Npas4); t(4)=18.3843 (Arc)); Fig. 8b (F(31)=2.701); Fig. 8c (F(31)=0.108); Fig. 8d (F(31)=0.2577); Fig. 8h (t(4)=1.4330 (LSD1); t(4)=3.9409 (LSD1c); t(4)=4.2848 (LSD1n)).

Also, the statistics are reported in Nature Neuroscience Reporting Checklist as supplemental information.

Analysis of alternative splicing of *LSD1*

Expression of *LSD1n* or *LSD1c* was analyzed using PCR or qPCR. cDNA templates from each sample were amplified using primer set jw493–494. PCR products were analyzed using 2% agarose gel, detecting *LSD1n* (91bp) or *LSD1c* (79bp). For qPCR method, *LSD1n* or *LSD1c* specific primers and common primers (primer set 1 or 2) were used to specifically amply *LSD1n* or *LSD1c* respectively.

Primer set jw493–494:

jw493:	GCCCACTTTATGAAGCCAATGGAC
jw494:	AGCAACCGGTTAAATTCTTGTTCT

Primer set 1:

jw771 (LSD1n specific):	TATGAAGCCAATGGACAAGCTGAC
jw772 (LSD1c specific):	TATGAAGCCAATGGACAAGCTGTT
jw773 (common):	ATGACAACCTCCAATGCCTGGCCA

Primer set 2:

jw774 (common):	GGTGGACGAGTTGCTACATTTCGA
jw775 (LSD1n specific):	TTCTTTTGGAACCTTGACAGTGTC
jw776 (LSD1c specific):	TTCTTTTGGAACAGCTTGTCCATT

Knockdown *Phf8* in cortical neurons using shRNA

Five Lentiviral shRNAs against mouse *Phf8* and control were purchased from Sigma MISSION shRNA library. Knockdown efficiency of each *Phf8* shRNA was determined and best two shRNAs (shPHF8-5 and shPHF8-7) were packaged and were used to infect mouse primary cortical neurons.

shPHF8-5: TRCN0000086825 NM_177201.2-734s1c1

Sequence: CCGG**GCAAGATGAAACTCGGTGATT**CTCGAG**AATCACCGAGTTTCATCTTGC**TTTTTG

shPHF8-7: TRCN0000086827 NM_177201.2-1504s1c1

Sequence: CCG**GCGGACTGTACAGCTCATTAAA**CTCGAG**TTTAATGAGCTGTACAGTCCG**TTTTTG

Primer sets for RT-qPCR

Mus musculus actin, beta, cytoplasmic (Actb), mRNA NM_007393

jw761: ACCTTCTACAATGAGCTGCGTGTG
jw762: CCTGGATGGCTACGTACATGGCTG

Mus musculus activity regulated cytoskeletal-associated protein (Arc), mRNA NM_018790

jw731: GAGCTGAAGCCACAAATGCAGCTG
jw732: TCATTCTCCTGGCTCTGTAGGCTC

Mus musculus B cell translocation gene 2, anti-proliferative (Btg2), mRNA NM_007570

jw905: GTTTTCAGTAGGGCGCTCCAGGAC
jw906: TGGTTGATACGGATACAGCGATAG

Mus musculus cysteine rich protein 61 (Cyr61), mRNA NM_010516

jw915: TCGGAGGTGGAGTTAACGAGAAAC
jw916: CGTGGTCTGAACGATGCATTTCTG

Mus musculus early growth response 1 (Egr1), mRNA NM_007913

jw745: GCAGCAGCGCCTTCAATCCTCAAG
jw746: GTCGTTTGGCTGGGATAACTCGTC

Mus musculus lysine (K)-specific demethylase 1A (Kdm1a), mRNA NM_133872

jw383: AGCAGCTCGACAGCTACAGAGTTT
jw384: TGGCGCCAAGATCAGCTACATAGT

Mus musculus neuronal PAS domain protein 4 (Npas4), mRNA NM_153553

jw903: GCTGTCCTACCTGCACATCATGAG
jw904: TGCCACAATGTCTTCAAGCTCTTG

Mus musculus proprotein convertase subtilisin/kexin type 1 (Pcsk1), mRNA NM_013628

jw823: CTATCAAGTCTCTGGAACATGTGC
jw824: GTATCTCTTTCCCTTTCAGCCAAC

Mus musculus PHD finger protein 8 (Phf8), mRNA NM_177201

jw769: TTTGCCAGACCACGAGGATGAGAT

jw770: TCACTGCCATCAAGGTCCATGTCT

Mus musculus supervillin (Svil), mRNA NM_153153

jw1091: CACTGAAAACAAGATAACCGGCTC

jw1092: AGCCCAGCATGAATAAGGTAAGAC

Primer sets for ChIP-qPCR

Mus musculus neuronal PAS domain protein 4 (Npas4), mRNA NM_153553

Npas4 5′ (−34 – 87)

jw1013: CTTCCTCTTCCTTGCTTCCCGGTC

jw1014: AGGAGCTATATAAGGCGGATCGAG

Npas4 3′ (2086 – 2190)

jw1017: GCGGTAGTGTTGAGAAGAAGCTTG

jw1018: GTCCTAATCTACCTGGGCTTTGAG

Mus musculus activity regulated cytoskeletal-associated protein (Arc), mRNA NM_018790

Arc 5′ (−3 – 95)

jw1021: TGCCGGAGGAGCTTAGCGAGTGTG

jw1022: GGTGCAGAGCTCAAGCGAGTTCTC

Arc 3′ (2012 – 2129)

jw1023: TGATGCCACTTCACTCCACCCTTG

jw1024: CCCTGCACCGTGTATCTTAGAGTG

Mus musculus early growth response 1 (Egr1), mRNA NM_007913

Egr1 5′ (−42 – 26)

jw1029: CTGTTCCAGACCCTTGAAATAGAG

jw1030: CCAAGTTCTGCGCGCTGGGATCTC

Egr1 3′ (2587 – 2673)

jw1031: GAGGCAGGAAAGACATAAAAGCAC

jw1032: TGGCTCTGAGATCTTCCATCTGAC

Primer sets for eRNAs

Npas4 eRNA plus strand:

jw965: CTCTGCGGTCAAATAACAAGACTG

jw966: GTCAGAGATGTCTAGGCCCAATAG

Arc eRNA plus strand:

jw1059: CTGGACCTCTTTCTTTCTCCGATG

jw1060: GGAGCTGGTTGTCAGTTTCAAAGC

Arc eRNA minus strand:

jw531: ATTTGGTGGCTGGTGTTCTGGATG

jw532: AGCCTCCCATGGCTCTTACTCATT

Fos eRNA1 plus strand:

jw573: GCACACAGACTTGGCAGGTTCAAA

jw574: AATGACGGGAACCAAACCAACAGC

Fos eRNA1 minus strand:

jw1053: CCTGAGAGCAGTGTTTATGGCTTC

jw1054: CAAGGGGAGAGAGAAATGAGGATG

Nr4a1 eRNA minus strand:

jw1067: GCTTAGGCACGGTAGTCATAGGAG

jw1068: CATAGTAGGCACTCAGACTTGGTC

Supplementary Material

Refer to Web version on PubMed Central for supplementary material.

Acknowledgments

We thank Dr. J. Chen at UCSD for pLNL vector for LSD1n gene targeting; Dr. S. Wu and Dr. M. Capecchi at University of Utah for pCAG-LSL vector for generation of *LSD1* transgenic mice. We thank Dr. J. Zhao and Dr. E. Kothari at UCSD transgenic core for generation of knockout and transgenic mice; Dr. S. Roberts at TSRI Mouse Behavioral Core for behavioral assessment; Dr. H. Karten at UCSD for brain anatomy analysis; Dr. M. Ghassemian at UCSD for MALDI-TOF mass spectrometry analysis; Drs. A. Gamliel, R. McEvilly, I. Garcia-Bassets, B. Bloodgood and CK. Glass at UCSD for discussion, comments, suggestions and critical reading of the manuscript; Ms. R. Pardee for proofreading of the manuscript; and Ms. J. Hightower for help with figures preparation. Dr. J. Wang was a recipient of NIH T32 Postdoctoral Fellowship. Dr. F. Telese was supported by grants from Roche Extending Innovation Network Program. Dr. W. Li was supported by a DoD postdoctoral fellowship. Dr. SL. Pfaff is Benjamin H. Lewis Chair in Neuroscience, an HHMI Investigator. Dr. MG. Rosenfeld is an HHMI Investigator. This research was supported by grants from NINDS (R37NS5037116) to SLP and by grants from NIH and NCI (DK018477, NS034934, DK039949, HL065445 and CA173903) to MGR.

References

1. Sweatt JD. The emerging field of neuroepigenetics. Neuron. 2013; 80:624–632. [PubMed: 24183015]
2. Borrelli E, Nestler EJ, Allis CD, Sassone-Corsi P. Decoding the epigenetic language of neuronal plasticity. Neuron. 2008; 60:961–74. [PubMed: 19109904]
3. Ronan JL, Wu W, Crabtree GR. From neural development to cognition: unexpected roles for chromatin. Nat Rev Genet. 2013; 14:347–59. [PubMed: 23568486]
4. Telese F, Gamliel A, Skowronska-Krawczyk D, Garcia-Bassets I, Rosenfeld MG. “Seq-ing” insights into the epigenetics of neuronal gene regulation. Neuron. 2013; 77:606–623. [PubMed: 23439116]

5. Andres ME, Burger C, Peral-Rubio MJ, Battaglioli E, Anderson ME, Grimes J, Dallman J, Ballas N, Mandel G. CoREST, a functional corepressor required for regulation of neural-specific gene expression. Proc Natl Acad Sci U S A. 1999; 96:9873–9878. [PubMed: 10449787]

6. Shi Y, Sawada J, Sui G, Affar el B, Whetstine JR, Lan F, Ogawa H, Luke MP, Nakatani Y, Shi Y. Coordinated histone modifications mediated by a CtBP co-repressor complex. Nature. 2003; 422:735–738. [PubMed: 12700765]

7. Shi Y, Lan F, Matson C, Mulligan P, Whetstine JR, Cole PA, Casero RA, Shi Y. Histone demethylation mediated by the nuclear amine oxidase homolog LSD1. Cell. 2004; 119:941–953. [PubMed: 15620353]

8. Metzger E, Wissmann M, Yin N, Müller JM, Schneider R, Peters AH, Günther T, Buettner R, Schüle R. LSD1 demethylates repressive histone marks to promote androgen-receptor-dependent transcription. Nature. 2005; 437:436–439. [PubMed: 16079795]

9. Garcia-Bassets I, Kwon YS, Telese F, Prefontaine GG, Hutt KR, Cheng CS, Ju BG, Ohgi KA, Wang J, Escoubet-Lozach L, Rose DW, Glass CK, Fu XD, Rosenfeld MG. Histone methylation-dependent mechanisms impose ligand dependency for gene activation by nuclear receptors. Cell. 2007; 128:505–18. [PubMed: 17289570]

10. Wang J, Scully K, Zhu X, Cai L, Zhang J, Prefontaine GG, Krones A, Ohgi KA, Zhu P, Garcia-Bassets I, Liu F, Taylor H, Lozach J, Jayes FL, Korach KS, Glass CK, Fu XD, Rosenfeld MG. Opposing LSD1 complexes function in developmental gene activation and repression programmes. Nature. 2007; 446:882–887. [PubMed: 17392792]

11. Zibetti C, Adamo A, Binda C, Forneris F, Toffolo E, Verpelli C, Ginelli E, Mattevi A, Sala C, Battaglioli E. Alternative splicing of the histone demethylase LSD1/KDM1 contributes to the modulation of neurite morphogenesis in the mammalian nervous system. J Neurosci. 2010; 30:2521–2532. [PubMed: 20164337]

12. Huang J, Sengupta R, Espejo AB, Lee MG, Dorsey JA, Richter M, Opravil S, Shiekhattar R, Bedford MT, Jenuwein T, Berger SL. p53 is regulated by the lysine demethylase LSD1. Nature. 2007; 449:105–108. [PubMed: 17805299]

13. Laurent B, Ruitu L, Murn J, Hempel K, Ferrao R, Xiang Y, Liu S, Garcia BA, Wu H, Wu F, Steen H, Shi Y. A Specific LSD1/KDM1A Isoform Regulates Neuronal Differentiation through H3K9 Demethylation. Molecular Cell. 2015; 57:957–970. [PubMed: 25684206]

14. Whyte WA, Bilodeau S, Orlando DA, Hoke HA, Frampton GM, Foster CT, Cowley SM, Young RA. Enhancer decommissioning by LSD1 during embryonic stem cell differentiation. Nature. 2012; 482:221–225. [PubMed: 22297846]

15. Kim TK, Hemberg M, Gray JM, Costa AM, Bear DM, Wu J, Harmin DA, Laptewicz M, Barbara-Haley K, Kuersten S, Markenscoff-Papadimitriou E, Kuhl D, Bito H, Worley PF, Kreiman G, Greenberg ME. Widespread transcription at neuronal activity-regulated enhancers. Nature. 2010; 465:182–187. [PubMed: 20393465]

16. Heinz S, Benner C, Spann N, Bertolino E, Lin YC, Laslo P, Cheng JX, Murre C, Singh H, Glass CK. Simple combinations of lineage-determining transcription factors prime cis-regulatory elements required for macrophage and B cell identities. Mol Cell. 2010; 38:576–89. [PubMed: 20513432]

17. Telese F, Ma Q, Perez PM, Notani D, Oh S, Li W, Comoletti D, Ohgi KA, Taylor H, Rosenfeld MG. LRP8-Reelin-regulated Neuronal (LRN) Enhancer Signature Underlying Learning and Memory Formation. Neuron. 2015; 86:696–710. [PubMed: 25892301]

18. Core LJ, Waterfall JJ, Lis JT. Nascent RNA sequencing reveals widespread pausing and divergent initiation at human promoters. Science. 2008; 322:1845–1848. [PubMed: 19056941]

19. Lin Y, Bloodgood BL, Hauser JL, Lapan AD, Koon AC, Kim TK, Hu LS, Malik AN, Greenberg ME. Activity-dependent regulation of inhibitory synapse development by Npas4. Nature. 2008; 455:1198–1204. [PubMed: 18815592]

20. Schaukowitch K, Joo JY, Liu X, Watts JK, Martinez C, Kim TK. Enhancer RNA Facilitates NELF Release from Immediate Early Genes. Mol Cell. 2014; 56:29–42. [PubMed: 25263592]

21. Nishioka K, Rice JC, Sarma K, Erdjument-Bromage H, Werner J, Wang Y, Chuikov S, Valenzuela P, Tempst P, Steward R, Lis JT, Allis CD, Reinberg D. PR-Set7 is a nucleosome-specific

methyltransferase that modifies lysine 20 of histone H4 and is associated with silent chromatin. Mol Cell. 2002; 9:1201–1213. [PubMed: 12086618]

22. Schotta G, Sengupta R, Kubicek S, Malin S, Kauer M, Callén E, Celeste A, Pagani M, Opravil S, Rosa-Velazquez IA, Espejo A, Bedford MT, Nussenzweig A, Busslinger M, Jenuwein T. A chromatin-wide transition to H4K20 monomethylation impairs genome integrity and programmed DNA rearrangements in the mouse. Genes & Development. 2008; 22:2048–2061. [PubMed: 18676810]
23. Qi HH, Sarkissian M, Hu GQ, Wang Z, Bhattacharjee A, Gordon DB, Gonzales M, Lan F, Ongusaha PP, Huarte M, Yaghi NK, Lim H, Garcia BA, Brizuela L, Zhao K, Roberts TM, Shi Y. Histone H4K20/H3K9 demethylase PHF8 regulates zebrafish brain and craniofacial development. Nature. 2010; 466:503–507. [PubMed: 20622853]
24. Liu W, Tanasa B, Tyurina OV, Zhou TY, Gassmann R, Liu WT, Ohgi KA, Benner C, Garcia-Bassets I, Aggarwal AK, Desai A, Dorrestein PC, Glass CK, Rosenfeld MG. PHF8 mediates histone H4 lysine 20 demethylation events involved in cell cycle progression. Nature. 2010; 466:508–12. [PubMed: 20622854]
25. Stender JD, Pascual G, Liu W, Kaikkonen MU, Do K, Spann NJ, Boutros M, Perrimon N, Rosenfeld MG, Glass CK. Control of proinflammatory gene programs by regulated trimethylation and demethylation of histone H4K20. Mol Cell. 2012; 48:28–38. [PubMed: 22921934]
26. Barski A, Cuddapah S, Cui K, Roh TY, Schones DE, Wang Z, Wei G, Chepelev I, Zhao K. High-resolution profiling of histone methylations in the human genome. Cell. 2007; 129:823–37. [PubMed: 17512414]
27. Saha RN, Wissink EM, Bailey ER, Zhao M, Fargo DC, Hwang JY, Daigle KR, Fenn JD, Adelman K, Dudek SM. Rapid activity-induced transcription of Arc and other IEGs relies on poised RNA polymerase II. Nat Neurosci. 2011; 14:848–856. [PubMed: 21623364]
28. Hargreaves DC, Horng T, Medzhitov R. Control of inducible gene expression by signal-dependent transcriptional elongation. Cell. 2009; 138:129–145. [PubMed: 19596240]
29. Kwak H, Lis JT. Control of transcriptional elongation. Annu Rev Genet. 2013; 47:483–508. [PubMed: 24050178]
30. Trojer P, Li G, Sims RJ 3rd, Vaquero A, Kalakonda N, Boccuni P, Lee D, Erdjument-Bromage H, Tempst P, Nimer SD, Wang YH, Reinberg D. L3MBTL1, a histone-methylation-dependent chromatin lock. Cell. 2007; 129:915–28. [PubMed: 17540172]
31. Yang Z, Yik JH, Chen R, He N, Jang MK, Ozato K, Zhou Q. Recruitment of P-TEFb for stimulation of transcriptional elongation by the bromodomain protein Brd4. Mol Cell. 2005; 19:535–45. [PubMed: 16109377]
32. West AE, Greenberg ME. Neuronal activity-regulated gene transcription in synapse development and cognitive function. Cold Spring Harb Perspect Biol. 2011; 3(6):a005744. [PubMed: 21555405]
33. Nam HJ, Boo K, Kim D, Han D, Choe HK, Kim CR, Sun W, Kim H, Kim K, Lee H, Metzger E, Schuele R, Yoo S, Takahashi JS, Cho S, Son GH, Baek SH. Phosphorylation of LSD1 by PKCα is crucial for circadian rhythmicity and phase resetting. Mol Cell. 2014; 53:791–805. [PubMed: 24582500]
34. Lee CT, Duerre JA. Changes in histone methylase activity of rat brain and liver with aging. Nature. 1974; 251:240–242. [PubMed: 4420569]
35. Evertts AG, Manning AL, Wang X, Dyson NJ, Garcia BA, Coller HA. H4K20 methylation regulates quiescence and chromatin compaction. Mol Biol Cell. 2013; 24:3025–3037. [PubMed: 23924899]
36. Schaefer A, Sampath SC, Intrator A, Min A, Gertler TS, Surmeier DJ, Tarakhovsky A, Greengard P. Control of cognition and adaptive behavior by the GLP/G9a epigenetic suppressor complex. Neuron. 2009; 64:678–91. [PubMed: 20005824]
37. Gupta-Agarwal S, Franklin AV, Deramus T, Wheelock M, Davis RL, McMahon LL, Lubin FD. G9a/GLP histone lysine dimethyltransferase complex activity in the hippocampus and the entorhinal cortex is required for gene activation and silencing during memory consolidation. J Neurosci. 2012; 32:5440–53. [PubMed: 22514307]

38. Beck DB, Oda H, Shen SS, Reinberg D. PR-Set7 and H4K20me1: at the crossroads of genome integrity, cell cycle, chromosome condensation, and transcription. Genes Dev. 2012; 26:325–37. [PubMed: 22345514]
39. Laumonnier F, Holbert S, Ronce N, Faravelli F, Lenzner S, Schwartz CE, Lespinasse J, Van Esch H, Lacombe D, Goizet C, Phan-Dinh Tuy F, van Bokhoven H, Fryns JP, Chelly J, Ropers HH, Moraine C, Hamel BC, Briault S. Mutations in PHF8 are associated with X linked mental retardation and cleft lip/cleft palate. J Med Genet. 2005; 42:780–6. [PubMed: 16199551]
40. Li W, Notani D, Ma Q, Tanasa B, Nunez E, Chen A, Merkurjev D, Zhang J, Ohgi K, Song X, Oh S, Kim H, Glass CK, Rosenfeld MG. Functional roles of enhancer RNAs for oestrogen-dependent transcriptional activation. Nature. 2013; 498:516–520. [PubMed: 23728302]
41. Wilhelm BT, Marguerat S, Watt S, Schubert F, Wood V, Goodhead I, Penkett CJ, Rogers J, Bähler J. Dynamic repertoire of a eukaryotic transcriptome surveyed at single-nucleotide resolution. Nature. 2008; 453:1239–1243. [PubMed: 18488015]
42. Sando R, Gounko N, Pieraut S, Liao L, Yates J, Maximov A. HDAC4 governs a transcriptional program essential for synaptic plasticity and memory. Cell. 2012; 151:821–834. [PubMed: 23141539]
43. Li X, Risbrough VB, Cates-Gatto C, Kaczanowska K, Finn MG, Roberts AJ, Markou A. Comparison of the effects of the GABAB receptor positive modulator BHF177 and the GABAB receptor agonist baclofen on anxiety-like behavior, learning, and memory in mice. Neuropharmacology. 2013; 70C:156–167. [PubMed: 23376712]
44. Lee HS, Ghetti A, Pinto-Duarte A, Wang X, Dziewczapolski G, Galimi F, Huitron-Resendiz S, Piña-Crespo JC, Roberts AJ, Verma IM, Sejnowski TJ, Heinemann SF. Astrocytes contribute to gamma oscillations and recognition memory. Proc Natl Acad Sci U S A. 2014; 111:E3343–52. [PubMed: 25071179]
45. Semenova S, Contet C, Roberts AJ, Markou A. Mice lacking the b4 subunit of the nicotinic acetylcholine receptor show memory deficits, altered anxiety- and depression-like behavior, and diminished nicotine-induced analgesia. Nicotine Tob Res. 2012; 14:1346–55. [PubMed: 22573727]
46. Bach ME, Hawkins RD, Osman M, Kandel ER, Mayford M. Impairment of spatial but not contextual memory in CaMKII mutant mice with a selective loss of hippocampal LTP in the range of the theta frequency. Cell. 1995; 81:905–915. [PubMed: 7781067]
47. Barnes CA. Memory deficits associated with senescence: a neurophysiological and behavioral study in the rat. J Comp Physiol. 1979; 93:74–104.
48. Eisen MB, Spellman PT, Brown PO, Botstein D. Cluster analysis and display of genome-wide expression patterns. Proc Natl Acad Sci U S A. 1998; 95:14863–8. [PubMed: 9843981]
49. Robinson MD, McCarthy DJ, Smyth GK. edgeR: a Bioconductor package for differential expression analysis of digital gene expression data. Bioinformatics. 2010; 26:139–140. [PubMed: 19910308]
50. Basnet H, Su X, Tan Y, Merkurjev D, Meisenhelder J, Ohgi KA, Hunter T, Pillus L, Rosenfeld MG. Tyrosine phosphorylation of histone H2A by CK2 regulates transcriptional elongation. Nature. 2014; 516:267–71. [PubMed: 25252977]

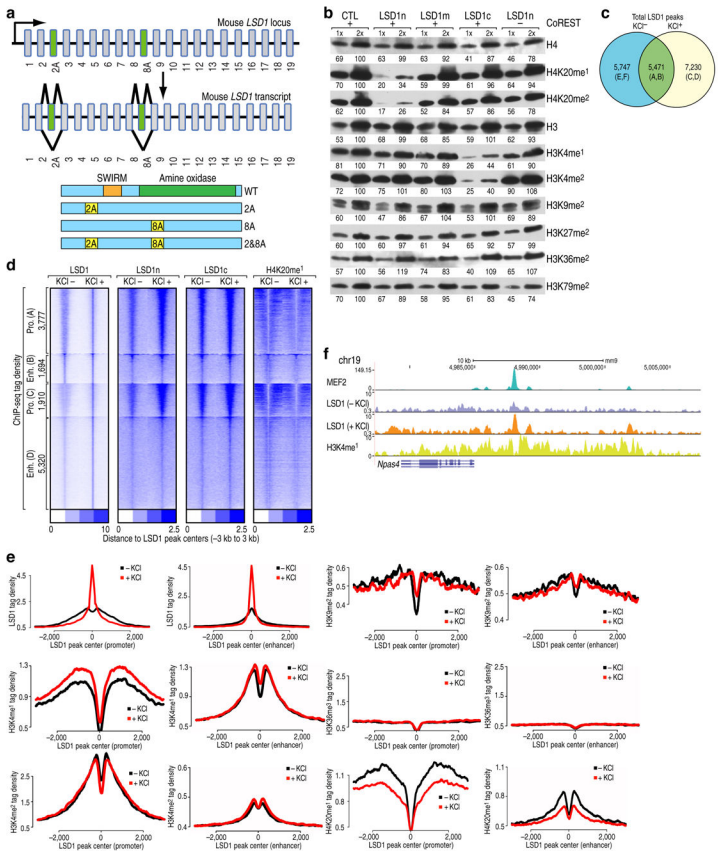

Figure 1. LSD1n removes H4K20 methylation *in vitro*

a) Diagram of alternative splicing events of *LSD1 gene*.

b) Histone demethylase assay *in vitro* using nucleosomes as substrates. Western blot analysis using antibodies against histone marks revealing removal of H4K20 methylation by LSD1n and enhanced in presence of CoREST. The amount of protein is quantified based on the intensity of the bands using ImageJ software, the 2x control has an arbitrarily assigned value of 100.

c) Venn diagram showing the genome-wide overlap of ChIP-seq peaks of LSD1 in primary cortical neurons before and after KCl-mediated depolarization (1 hour). A, C, D sites indicate promoters and B, D, F indicate enhancers reported in Fig. 1D.

d) LSD1 genome occupancy in cortical neurons is changed after KCl-mediated depolarization. Heatmaps display LSD1 (total), FLAG-LSD1c, FLAG-LSD1n and H4K20me1 genome occupancies before and after KCl treatment (1 hour) in cortical neurons, centered on LSD1-peaks in −KCl and divided in 4 groups based on Fig. 1C Additional 3kb from the center of the peaks is shown.

e) Histogram plots of normalized ChIP-seq tag intensities of LSD1, H3K4me1, H3K4me2, H3K9me2, H3K36me3 and H4K20me1 in cortical neurons, centered on gained LSD1-peaks at promoters and enhancers before and after KCl treatment (1 hour). Additional 2kb from the center of the peaks is shown.

f) UCSC genome browser image of *Npas4* locus, revealing overlapping MEF2 and LSD1 peaks.

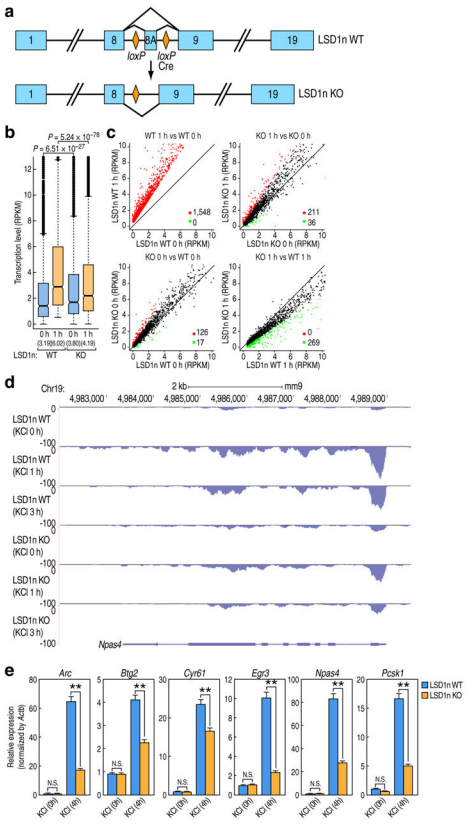

Figure 2. LSD1n is required for neuronal activity-regulated gene transcription

a) Schematic diagram of the generation of *LSD1n* knockout mice;

b) Neuronal activity-dependent gene expression is compromised in *LSD1n* KO primary cortical neurons assessed by GRO-seq. Box-and-whisker plots of gene expression level (RPKM) in WT and *LSD1n* KO neurons before and after KCl treatment (1 hour). P-values denote statistic differences between treatment conditions (p=6.51E-27 at 0hr; p=5.24E-78 at 1hr; n=1548 number of genes up-regulated in WT control neurons, paired t-test).

c) Scatter plots of gene expression (RPKM) in WT and *LSD1n* KO primary cortical neurons before and after KCl-mediated depolarization (1 hour).

d) Neuronal activity-regulated *Npas4* gene expression is compromised in *LSD1n* KO primary cortical neurons assessed by GRO-seq. UCSC genome browser image showing *Npas4* locus.

e) RT-qPCR indicating that neuronal activity-dependent gene expression is compromised in *LSD1n* KO cortical neurons. RNA was analyzed before and after KCl treatment (4 hours). Data are normalized against *Actb.* Data are shown as mean ± SD; N.S.= non-statistically significant (p=0.004 Arc; p=0.003 Btg2; p=0.032 Cyr61; p=0.001 Egr3; p=0.011 Npas4; p=0.016 Pcsk1; n=3 technical replicates from a pool of 8–12 embryos; unpaired t-test).

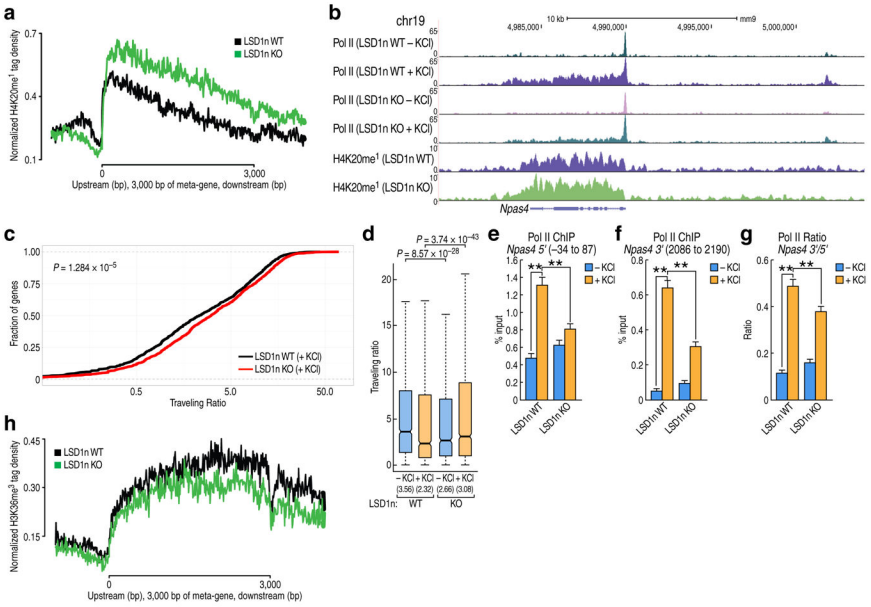

Figure 3. LSD1n removes H4K20 methylation *in vivo* and promotes transcriptional elongation

a) LSD1n removes H4K20me *in vivo*. Histogram plots of normalized ChIP-seq tag intensities of H4K20me1 in WT and *LSD1n* KO cortical neurons on transcribed coding regions of neuronal activity-regulated genes, revealing increased level of H4K20me1 in *LSD1n* KO cortical neurons.

b) *Npas4* gene expression is regulated at LSD1n-dependent transcriptional elongation steps assessed by RNA Pol II ChIP-seq. UCSC genome browser image showing of *Npas4* locus.

c) Neuronal activity-regulated gene transcription elongation is LSD1n-dependent assessed by RNA Pol II ChIP-seq. RNA Pol II traveling ratio plots is calculated for the fraction of neuronal activity-regulated genes in WT and *LSD1n* KO cortical neurons. P-values denote statistic differences between WT and *LSD1n* KO cortical neurons (p=1.284E-05, n=1548 up-regulated genes; two-tailed KS test);

d) Neuronal activity-dependent gene transcription elongation is LSD1n-dependent assessed by RNA Pol II ChIP-seq. Box-and-whisker plots of traveling ratio for neuronal activity-regulated genes in WT and *LSD1n* KO cortical neurons before and after KCl-mediated depolarization (1 hour). P-values denote statistic differences between WT and *LSD1n* KO cortical neurons (p=8.57E-28 at 0hr; p=3.74E-43 at 1hr, n=1548 up-regulated genes; paired t-test);

e) RNA Pol II ChIP showing RNA Pol II recruitments on *Npas4* 5′ region (TSS). Data are shown as mean ± SD; ** = P-value <0.01 (p=0.0002; p=0.0009, n=4 technical replicates from a pool of 8–12 embryos; unpaired t-test);

f) RNA Pol II ChIP showing RNA Pol II recruitments on *Npas4* 3′ region (coding region). Data are shown as mean ± SD; ** = P-value <0.01 (p=5.4E-6; p=0.0004, n=4 technical replicates from a pool of 8–12 embryos; unpaired t-test);

g) RNA Pol II ChIP showing that elongation of RNA Pol II on *Npas4* coding region was comprised (decreased 3′/5′ ratio) in *LSD1n* KO cortical neurons after KCl-mediated depolarization (1 hour). Data are shown as mean ± SD; ** = P-value <0.01 (p=0.0002; p=0.0091, n=4 technical replicates from a pool of 8–12 embryos; unpaired t-test);

h) LSD1n is required for transcription elongation assessed by H3K36me3 ChIP-seq experiments. Histogram plots of normalized ChIP-seq tag intensities of H3K36me3 in WT and *LSD1n* KO cortical neurons on transcribed code regions of neuronal activity-regulated genes, revealing decreased level of H3K36me3 in *LSD1n* KO cortical neurons.

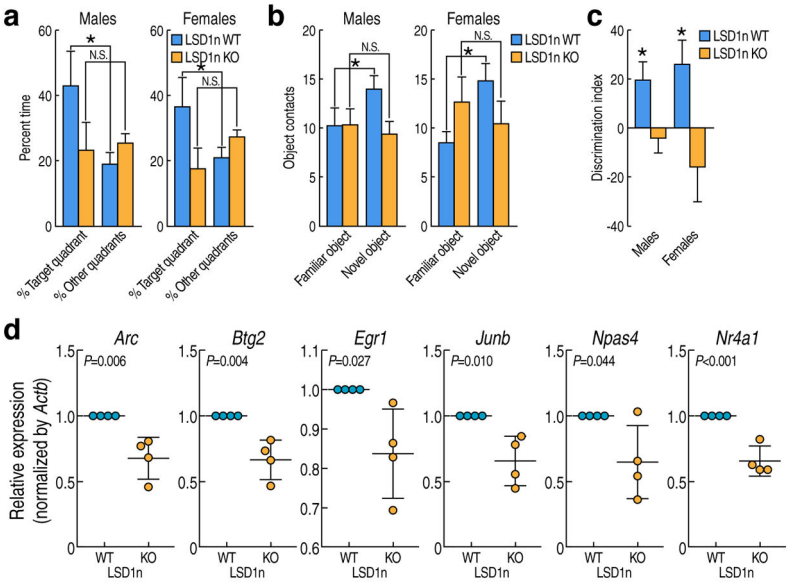

Figure 4. LSD1n is required for learning and memory

a) Schematic diagram of Barnes maze behavioral test. Histograms showing percent time spent in quadrants by male or female WT and *LSD1n* KO mice, revealing impaired spatial memory in *LSD1n* KO mice. N.S.= non-statistically significant, * = P-value<0.05 (p=0.0379 WT; p=0.3848 KO, n=10 number of age-matched mice/group; One-way ANOVA test);

b) Schematic diagram of novel object recognition test. Histograms showing number of object contacts identified by male or female WT and *LSD1n* KO mice, revealing impaired long-term memory in *LSD1n* KO mice. N.S.= non-statistically significant, * = P-value<0.05 (p=0.0013 WT; p=0.3180 KO, n=10 number of age-matched mice/group; One-way ANOVA test);

c) Histogram showing discrimination index calculated from the novel object recognition test results for male or female WT control and *LSD1n* KO mice, revealing impaired long-term memory in *LSD1n* KO mice. * = P-value<0.05 (p=0.0015 WT; p=0.7961 KO, n=10 number of age-matched mice/group; One-way ANOVA test);

d) RT-qPCR showing gene expression levels of *Arc*, *Btg2*, *Egr1*, *Junb*, *Npas4* and *Nr4a1* in cortex of WT control and *LSD1n* KO mice. Data are shown as mean ± SD. P-values denote differences between WT and KO (p=0.006092474 Arc; p=0.003948391 Btg2; p=0.02661944 Egr1; p=0.010277144 Junb; p=0.044014923 Npas4; p=0.000765615 Nr4a1; n=4 technical replicates from a pool of 8–12 embryos; unpaired t-test).